Spectroscopic Analysis of Chain Conformation of Poly(propylene oxide)-Based Polymer Electrolytes

Sunghoe Yoon, Kimio Ichikawa, William J. MacKnight, and Shaw Ling Hsu*

Polymer Science and Engineering Department, and Materials Research Science and Engineering Center, University of Massachusetts, Amherst, Massachusetts 01003

Received September 19, 1994; Revised Manuscript Received March 20, 1995®

ABSTRACT: Fourier transform Raman spectroscopy has been utilized, in combination with normal coordinate analysis, to characterize chain conformational changes of amorphous poly(propylene oxide) (PPO) when used as a matrix for polymer electrolytes. Our data indicate that in the presence of salt, poly(propylene oxide) displays a characteristic Raman band at 810 cm^{-1} increasing in intensity with an increase in $LiClO_4$ concentration. 1,2-Dimethoxypropane (DMP) was found to be an excellent model for data interpretation. Both the intensity and frequency of Raman active 1,2-dimethoxypropane vibrations were calculated. The C−C or C−O bands in the 700−900 cm^{-1} region were found to be particularly sensitive to chain conformational changes. The bands at 810 and 836 cm^{-1} were assigned to $TG_{\alpha}T$ and TTT conformations of the −O−C−C−O− sequence along the backbone, respectively. Therefore an increase in intensity at 810 cm^{-1} directly correlates to an increase in the $TG_{\alpha}T$ conformation with an increase in salt concentration. The effects of end groups on chain conformational changes were also studied since Li^+ can interact with both −OH end groups and ether oxygens. Poly(propylene oxide)s having hydroxy and methoxy end groups were compared. Our analyses indicate the interaction between hydroxy end groups and the lithium cation does not contribute as significantly to formation of the $TG_{\alpha}T$ conformation as does the interaction between the ether oxygen and lithium cation.

Introduction

Polymer electrolytes possess better dimensional, thermal, and chemical stability than inorganic and solution electrolytes.[1,2] The host polymer in polymer electrolytes usually consists of highly polar atoms which can solvate various ions. In such systems, the structure of the polymer matrix is extremely important since ionic conduction is governed by local segmental motions of the polymer chain as well as the number of free ions.[3−8] Typically-used polymers include polyethers such as poly(propylene oxide) or poly(ethylene oxide) (PEO), as various ions are highly soluble in these polymers. This characteristic can be attributed to specific interactions between the ether oxygen and the cations utilized.[1,9] This solvation property can be altered by polymer structure, since it has been shown that poly(ethylene oxide) exhibits much better solvating power for many salts than either poly(methylene oxide) [$-CH_2-O-$] or poly(trimethylene oxide) [$-CH_2CH_2CH_2-O$].[1] The differences have been shown to be correlated to spacing of polar atoms along the chain. Furthermore, the lower ionic conductivity of PPO-based rather than PEO-based electrolytes has been attributed to the steric hindrance caused by the $-CH_3$ side group interfering with the interaction between the ether oxygen and cation.[10] Undoubtedly, a better understanding of the chain conformational distribution of the host polymer will lead to a better understanding of the ionic conduction mechanism.

Vibrational spectroscopy, both infrared and Raman, has been used to characterize conformational changes induced by polymer−salt interactions. A number of studies have focused particular attention on characterization of poly(ethylene oxide) conformational changes with introduction of salts.[11−15] However, although several spectroscopic studies have been conducted, very limited quantitative structural analysis has been carried out for poly(propylene oxide)-based polymer electrolytes.[16−20] Raman active bands are strongly dependent on the polarizability changes of C−C bonds along the backbone and can be extremely sensitive to chain conformational changes.[21] Low-frequency Raman bands observed for poly(propylene oxide)-based electrolytes have considerable contributions from CCO/COC skeletal-bending coordinates and can be sensitive to chain conformational changes. These bands exhibit significant frequency shifts and bandwidth changes as a function of salt concentration.[16] The frequency shifts have been interpreted in terms of changing chain stiffness.[20] There are also other new unexplained spectroscopic features present when salts are introduced, and a detailed interpretation of poly(propylene oxide) structure in the presence of salts has yet to emerge. The vibrational spectra for a specific chain conformation can be analyzed. However, since the poly(propylene oxide) used for polymer electrolytes has a disordered structure, the obtained vibrational spectra generally consist of overlapping features associated with many different chain conformations.

Since the early '60s, theoretical normal vibrational analysis, based on the solution of the harmonic equation of motion which provides a set of frequencies and eigenvectors, has been extensively used to better understand polymer infrared and Raman spectra. Such analysis, typically accomplished by use of Wilson's GF matrix method and force constants transferred from small molecules, is applicable only for a specific chain conformation.[22,23] Snyder and co-workers recently developed a set of programs capable of reproducing observed vibrational spectra for both ordered and disordered oligomeric systems.[24] Chain conformation is generated on the basis of the rotational isomeric state model with the specific number of isomeric states governed by the energy differences of the states. With a surprisingly small number of parameters, it has been possible to reproduce remarkably accurate experimental

* To whom correspondence should be sent.
® Abstract published in *Advance ACS Abstracts,* May 15, 1995.

0024-9297/95/2228-4278$09.00/0

Table 1. Hydroxy Content Determined for HPPO

MW	−OH no. (mg of KOH/g)[a]	MW	−OH no. (mg of KOH/g)[a]
425		3000	35.24
1000	111.85	4000	26.94
2000	55.56		

[a] Determined by titration based on ASTM D4274.

infrared and Raman spectra of disordered chains. Snyder and co-workers analyzed the low-frequency (0−600 cm^{-1}) Raman spectra of *n*-alkanes in the liquid state.[24] Subsequently, this method was applied for analysis of the low-frequency Raman spectrum of molten state isotactic polypropylene and successfully demonstrated that the vibrational spectroscopic analysis can be used to identify the correct model governing the chain.[25] This method has been extended to analysis of higher frequency vibrations (0−1500 cm^{-1}) of liquid *n*-alkanes.[21]

To reduce the complexity of our analysis, 1,2-dimethoxypropane has been utilized as a model compound for poly(propylene oxide). The spectral change obtained for the model compound by salt addition remarkably resembles that obtained for poly(propylene oxide). 1,2-Dimethoxypropane has the same structure as the chemical repeat unit of poly(propylene oxide).[26] In addition, conformational analysis has revealed that the conformer distribution obtained for 1,2-dimethoxypropane was no different from that of the C−C bond along the poly(propylene oxide) chain, even though long range interactions are not considered.[26] Although it is difficult to characterize a disordered polymer state utilizing information obtained from a small molecular model, some vibrational modes are sufficiently localized to be used for analysis of common spectroscopic features in both the model and polymer. By analyzing experimental data in conjunction with normal coordinate analysis, chain conformational changes of poly(propylene oxide) in the presence of salts can be obtained. Our results are reported herein.

Materials and Experiment

Hydroxy-terminated poly(propylene oxide) (HPPO) samples of molecular weights 425 (HPPO 425), 1000 (HPPO 1000), and 4000 (HPPO 4000) were obtained from Aldrich Chemical Co. The hydroxy content (Table 1) was determined by titration (ASTM D4274). Extreme care was exercised to prevent water contamination during sample preparation. HPPO samples received were dried under high vacuum at 70 °C. Lithium perchlorate obtained from Aldrich was also dried at 150 °C under high vacuum for 1 day, dissolved in fresh dried THF (Aldrich) and added to the dried HPPO under dry argon gas in a glovebag. The solvent was removed at 60 °C, stored for 2 days under vacuum, and then further dried at 100−130 °C at high vacuum depending on the HPPO molecular weight. Lastly, all samples were dried at room temperature for an additional week at high vacuum. Lithium perchlorate/HPPO complexes were prepared with compositions of $[Li^+]$/[propylene oxide unit] = 0.05, 0.10, 0.15, and 0.20. 1,2-Dimethoxypropane was used as received from Aldrich. Lithium-complexed 1,2-dimethoxypropane was prepared by dissolving $LiClO_4$ directly into 1,2-dimethoxypropane.

Methoxy-terminated poly(propylene oxide) (MPPO) was prepared in order to examine end group effects. We selected the two lowest HPPO's of molecular weights 425 and 1000, as the largest end group effects are expected for these samples. The reaction flask containing dried HPPO was connected under dry argon gas to a condenser equipped at the top with a drying agent. The HPPO's had been treated with NaH (Aldrich, 95%) for 1 day. Excess CH_3I was added by syringe into the flask and the reaction mixture allowed to stand for another day. The NaH residue was killed by MeOH and the mixture separated to MPPO and other side products and impurities by separatory fractionation. MPPO was obtained as a yellow transparent liquid.

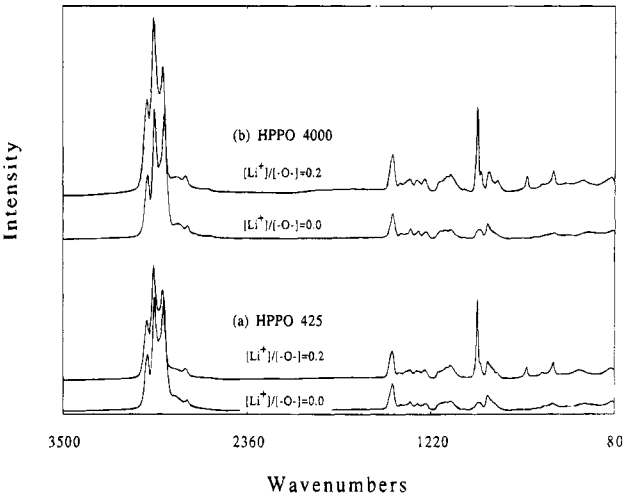

Figure 1. Fourier transform Raman spectra of HPPO and HPPO/$LiClO_4$ complex. The spectral resolution was maintained at 4 cm^{-1}. The laser power was maintained at 500 mW at the sample.

Hydroxy groups were not detected in the FT-IR spectrum obtained at room temperature by use of an IBM 38 system equipped with a dry nitrogen line and DTGS detector. The FT-IR spectrum was obtained with samples pressed between two potassium bromide plates. A total of 128 scans were signal averaged at a spectral resolution of 2 cm^{-1}. Use of a Bruker FT-NMR (200 MHz) provided no significant peak indicative of hydroxy groups. The ratio of the number of hydrogens of CH_3 in CH_3−O− units and CH_3−C− units calculated by integrating the area under the peaks was obtained as expected for perfect substitution. By use of a GPC equipped with polystyrene columns and a differential refractometer (Waters), it was confirmed that there is no change in the polydispersity index, thus indicating no polymer degradation. Finally, microanalysis provided no indication of the presence of sodium and iodine. $LiClO_4$-complexed MPPO's were prepared by the same procedure utilized for preparation of salt-complexed HPPO's.

It is interesting to note that the complexation of MPPO with salt is more complex than HPPO salt complexes in that a two-layer macroscopic phase separation occurred for the MPPO/$LiClO_4$ complex. From Raman spectroscopy, differential scanning calorimetry (DSC), and microanalysis, the upper layer was found to consist of pure MPPO. The bottom layer consists of MPPO complexed with added salt. It is also interesting to note that the amount of salt in this fraction is independent of initial salt concentration. The composition of the lower layer was found to be constant at $[Li^+]/[-O-] = 0.15 \pm 0.02$. This phase-separated structure, controlled by the relative strength of the specific binding energy between the lithium cation and ether unit and distributed long-range Coulombic interaction of the system, has been observed and analyzed in previous studies.[10]

Dispersive Raman data were difficult to obtain since some samples exhibit fluorescence using laser excitation in the visible region. This difficulty is largely overcome by use of long wavelength excitation in Fourier transform Raman spectroscopy. The spectra were obtained at room temperature using a Bruker FRA 106 spectrometer. A Nd:Yag laser with a wavelength of 1064 nm was used as excitation. The laser output power was maintained at 500 mW. A total of 1024 scans were loaded to obtain an enhanced signal to noise ratio. The excitation collection geometry was 180°, and spectral resolution was maintained at 4 cm^{-1}.

Raman spectra were obtained for HPPO's of molecular weights 425, 1000, 2000, 3000, and 4000. All samples exhibit identical features in the observed Raman spectra. Therefore, we report only the spectra obtained for the two extreme molecular weights. Figure 1 presents Raman spectra of HPPO

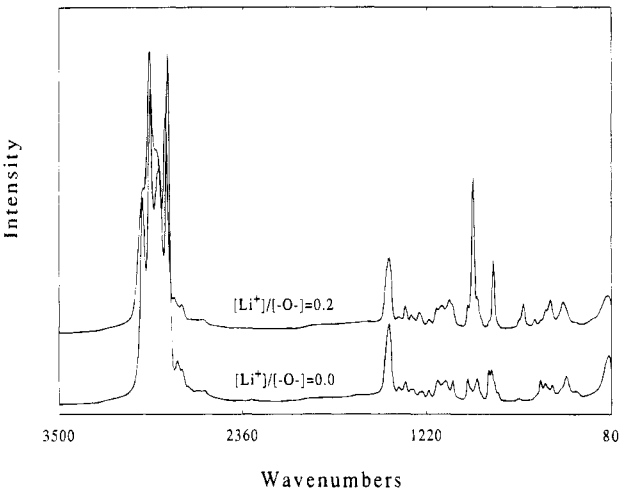

Figure 2. Fourier transform Raman spectra of 1,2-dimethoxypropane and DMP/$LiClO_4$ complex in the 80−3500 cm^{-1} region.

425 and HPPO 4000 and their salt complexes. Similar Raman data obtained for 1,2-dimethoxypropane and its salt complexes are shown in Figure 2. One interesting region showing spectral changes is that between 700 and 900 cm^{-1}.[20] The spectra obtained for 1,2-dimethoxypropane, HPPO, and their salt complexes are shown in Figure 3.

Normal Vibrational Analysis

As mentioned previously, changes in chain conformations are expected to be reflected in the relative intensity of specific Raman active vibrations. This has indeed been shown to be the case. In earlier studies, emphasis was devoted to characterization of vibrational modes associated with specific chain conformations.[27-31] Recently, using very few parameters and chain conformational distributions based on generally accepted rotational isomeric states, Snyder and co-workers analyzed both the frequency and intensity of spectra expected for a broad distribution of chain conformations. The success of this method has been demonstrated for completely amorphous systems such as liquid *n*-alkanes or molten isotactic polypropylene.[21,24,25] A similar analysis was applied to our system.

For numerical analysis of 1,2-dimethoxypropane as a model compound, we considered the three energy minimum states suggested for the propylene oxide unit. Newman projections of the three states are given in Figure 4 for the (*S*)-configuration of the chiral carbon. Among the three lowest energy states, the gauche α conformation has been suggested to be the most stable for both 1,2-dimethoxypropane and poly(propylene oxide) and is attributed to the "gauche oxygen effect".[32-34] Since our experiments reveal great similarity between the spectra obtained for 1,2-dimethoxypropane and poly(propylene oxide) when both form salt complexes, an analysis of the 1,2-dimethoxypropane vibrational spectrum can be used to explain spectral changes occurring in poly(propylene oxide) in the presence of salt.

The number of normal modes expected for each 1,2-dimethoxypropane conformer is 51. In our analysis, all bond angles were assumed to be tetrahedral. C−H, C−O, and C−C bond lengths were assumed to be 1.096, 1.41, and 1.54 Å, respectively.[35] The computer program used in this study has been described earlier.[21,24,25,27,28,31,35-39] The dihedral angles associated with the trans, gauche α, and gauche β states are assigned to +180, +60 and −60°, respectively, at the beginning of each calculation. A conformational distribution is then generated on the basis of the statistical weight expected for the final distribution of the structure. Variations of 5° were used to simulate fluctuations associated with each dihedral angle. The orientation of the end and side methyl groups is fixed. The number of conformers used in the calculation was 3000.

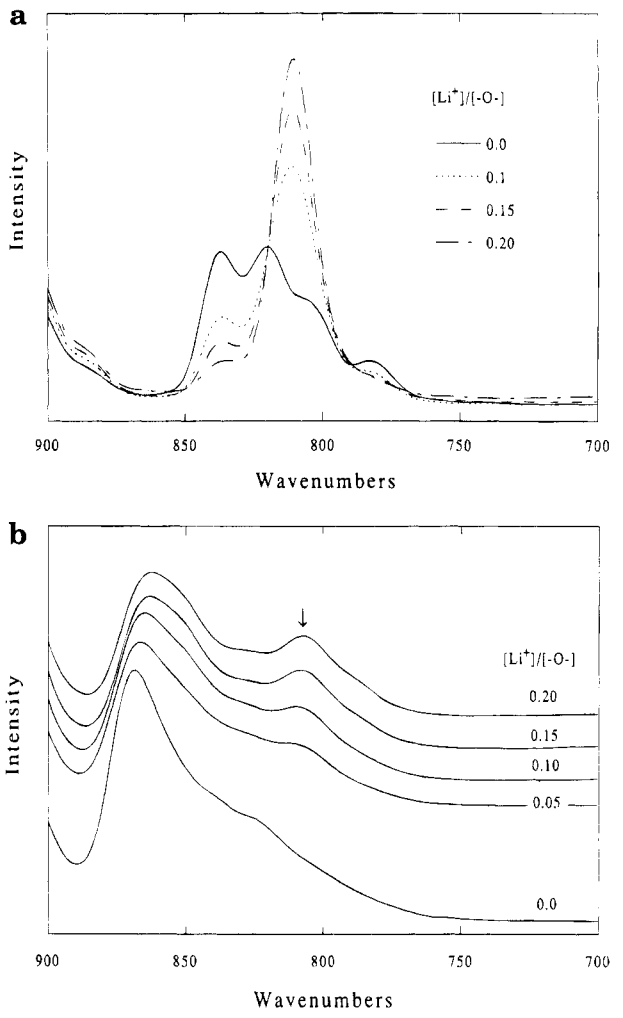

Figure 3. Fourier transform Raman spectra over the region between 700 and 900 cm^{-1} with $[Li^+]/[-O-] = 0-0.2$: (a) DMP; (b) HPPO 4000.

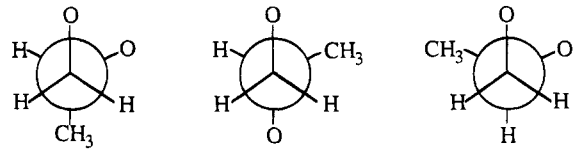

Figure 4. Newman projections of the three energy minimum states suggested for 1,2-dimethoxypropane and poly(propylene oxide) for the (*S*)-configuration.

The isotropic Raman spectrum, $S(\nu)$, of 1,2-dimethoxypropane can be approximated by summation of the spectrum, $S^C(\nu)$, of an individual conformer *C*.

$$S(\nu) \propto \sum_{C=1}^{C_T} S^C(\nu) \qquad (1)$$

where ν is frequency. Each conformer *C* is generated by the probability of each conformation assigned to each bond of obtaining the final conformational distribution. C_T is the total number of conformers, i.e. 3000 in our

Table 2. Corrections to the Earlier Force Field Used To Calculate Small Ether Systems

force constant	group	coordinates[a] and values	corrected coordinates and values
$H\alpha$	CH_3–C	∠HCC, 0.540	∠HCH, 0.540
$F\sigma$	CH_3–O	∠HCO, ∠HCO, −0.023	∠HCO, ∠HCO, −0.029
$f_{\mu\theta}{}^g$	CH–O–C	∠HCO, ∠COC, 0.004	∠HCO, ∠COC, −0.112
$f_{\mu\theta}{}^t$	CH–O–C	∠HCO, ∠COC, −0.112	∠HCO, ∠COC, 0.004

[a] *Spectrochim. Acta* **1967**, *23A*, 391 (Table 7).

calculation. The conformational probability, i.e. energy difference between trans and gauche conformers of each 1,2-dimethoxypropane bond, is adjusted until the most similar Raman spectrum as compared with the experimental result is obtained.

The set of valence force fields used in our calculation was obtained from an earlier study of 10 simple ether systems.[35] To validate the current program used for our ether system, vibrational spectra for methyl isopropyl ether and dimethyl ether were calculated and compared to the earlier study. Upon applying corrected nomenclature for some force constants presented previously, the earlier results were duplicated. The corrections for the force constants are summarized in Table 2.

Our analysis of the calculated Raman spectrum indicates that the C–C and C–O stretching vibrations are the most significant contributors to the isotropic Raman intensity in the range 700–900 cm^{-1}. Other internal coordinates, such as CH_2 rocking, certainly couple to these stretching coordinates. Their polarizability changes are generally quite small. Their contributions to the overall intensity can thus be ignored.[21,29,40] The scattering activity of the kth normal mode can then be given by the expression

$$S_k \propto [\sum_i \bar{\alpha}'_{CC} L_{ik} + \sum_j \bar{\alpha}'_{CO} L_{jk}]^2 \qquad (2)$$

where L_{ik} is the normal coordinate element for the ith C–C stretching internal coordinate and L_{jk} is that for the C–O stretching coordinate, α'_{CC} and α'_{CO} are the mean polarizability derivatives associated with C–C and C–O stretching, respectively. The mean polarizability derivative ratio of the C–C to C–O stretch used in this calculation is 2:1. Since the intensity parameters associated with the ether oxygen are not well established, we have determined that ratio on the basis of the bond polarizability values transferred from methyl vinyl ether and alkanes.[41,42] The values used give the best fit to the data measured. These values are assumed to be insensitive to changes in chain conformation.[21,43] The temperature effects on the occupation probability of various vibrational levels are extremely small for bands in this region and therefore not considered. The calculated spectra are expressed in terms of scattering activity by giving to each frequency a Lorentzian band shape having a FWHM (full width at half-maximum) of 8 cm^{-1}.[24] We have determined that $I_\perp$ has only limited intensity in the 800 cm^{-1} region. Therefore, we assume that the isotropic Raman spectrum can be approximated to the unpolarized spectra obtained in our Fourier transform instrument.

Results and Discussion

As seen in Figure 3, the bands in the 700–900 cm^{-1} region are broad and ill defined in the absence of salt. However, an obvious change in intensity at 810 cm^{-1} is observed with increasing salt concentration. As shown in Table 3, these band frequencies are independent of molecular weight and therefore must be sufficiently localized to reflect a localized vibrational mode. Although this observation has been mentioned previously,[20] to our knowledge no explanation has been proposed regarding these spectroscopic changes. A new weak shoulder at ca. 851 cm^{-1} appeared in the HPPO/salt complex, as seen in Figure 3.

HPPO and 1,2-dimethoxypropane exhibit significantly different intensity changes as a function of $LiClO_4$ salt concentration. The changes are more dramatic in 1,2-dimethoxypropane than in HPPO. The intensity at 810 cm^{-1} normalized to the 624 cm^{-1} assignable to the perchlorate anion for HPPO's by changing the molecular weight is shown in Figure 5. The intensity change is seen to be molecular weight dependent, increasing linearly with increasing chain length. However, the largest change at that particular band observed for 1,2-dimethoxypropane compared with any other HPPO system is contradictory to this molecular weight dependence. It is possible then that there is a contribution from specific interactions between the ions introduced and the hydroxy end groups of HPPO's.

The effect of hydroxy end groups was then evaluated by analyzing methoxy-substituted PPO's (MPPO). In this study of end group effects, as described above, we have synthesized MPPO's of molecular weights 425 and 1000. These lower molecular weights of PPO's were chosen because larger end group effects were expected in comparison to PPO's of higher molecular weights. As end effects are expected to dominate for HPPO of the lowest molecular weight, we have reported the observed spectra. The Raman spectra of pure MPPO of molecular weight 425 and its salt-complexed MPPO are shown in Figure 6. Similar to changes observed in the DMP/$LiClO_4$ system, the significant intensity change occurs in the 800 cm^{-1} region. Unlike HPPO of the same molecular weight, the 810 cm^{-1} band becomes dominant in the salt-complexed MPPO. Since the lithium cation can interact with hydroxy groups as well as the ether oxygen, this difference between MPPO and HPPO salt complexes indicates that the intensity change at 810 cm^{-1} results from interaction between the lithium cation and ether oxygen. Also, the molecular weight dependence of the band intensity at 810 cm^{-1} can be explained in terms of the relative content of hydroxy groups. Again, a new band was observed at 853 cm^{-1} in salt-complexed MPPO, as observed in salt-complexed HPPO. An explanation for that spectral change is not available at this point.

The calculated isotropic Raman spectra of a chain having certain conformational distribution and one for the $TG_\alpha T$ conformation along the –O–C–C–O– bond of (*S*)-DMP are shown in Figure 7. Three bands at 835, 817, and 807 cm^{-1} are calculated for the conformational distribution in Figure 7. A single band at 812 cm^{-1} is calculated for the $TG_\alpha T$ conformation. On the basis of analysis of the characteristics of normal modes, the lowest frequency component at 807 cm^{-1} (or 812 cm^{-1}) is attributed to the trans (O–C)–gauche α (C–C)–trans (C–O) ($TG_\alpha T$) conformation. The band centered at 817 cm^{-1} has contributions from molecules associated with $G_\alpha G_\alpha T$ and/or $G_\beta G_\alpha T$ structures. In good agreement with a previous study,[44] the main contributor to the band at 835 cm^{-1} was the trans (O–C)–trans (C–C)–trans (C–O) conformation of the –O–C–C–O– bond. On the basis of comparison of the relative intensity of the bands associated with different conformations, we

Table 3. Energy (Wavenumbers) at ~810 cm^{-1} Dependence on Salt Concentration and Chain Length

	wavenumber (cm^{-1})					
[Li$^+$]/[−O−]	DMP	HPPO425	HPPO1000	HPPO4000	MPPO425	MPPO1000
0.0	807				807	
0.05	813	810 (sh)[b]	808 (sh)	810 (sh)		
0.10	811	810	808	809		
0.13[a]						809
0.15	811	810	808	808		
0.17[a]					810	
0.20	811	809	808	807		

[a] Determined by microanalysis for the lower layer of salt-complexed MPPO. [b] sh: shoulder.

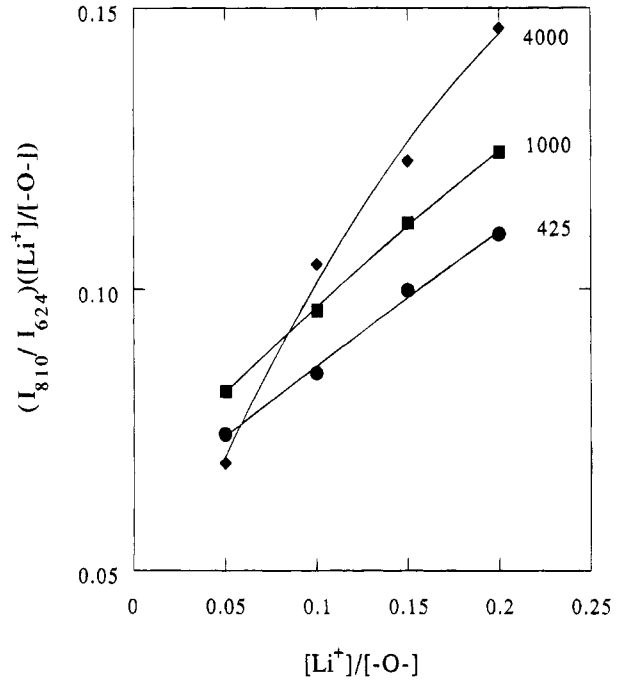

Figure 5. Li$^+$ concentration dependence of the intensity at ~810 cm^{-1} for different molecular weights of HPPO.

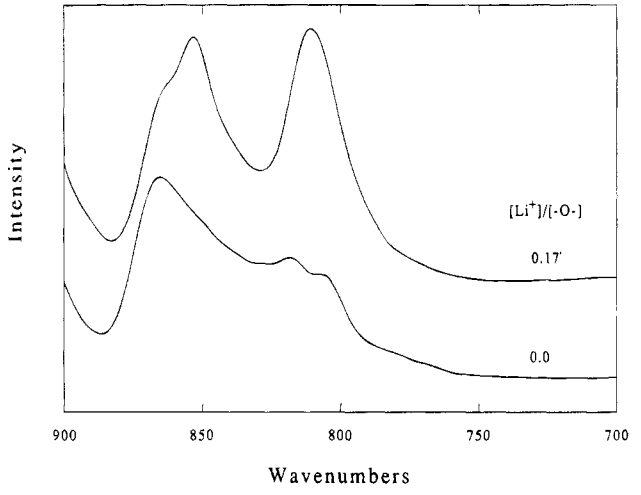

Figure 6. Fourier transform Raman spectra of uncomplexed MPPO and $LiClO_4$-complexed MPPO (the lower layer after phase separation) in the 700−900 cm^{-1}. MW of MPPO = 450.

conclude that $E_{g\alpha}$ associated with the C−C is an extremely low value of ~120 cal/mol relative to that of the trans conformer. The energy difference is smaller than the measured value of 1,2-dimethoxypropane in the gaseous phase.[32,34] Once polarizability tensors are determined from earlier studies,[41,42] there are no additional adjustable parameters available to better fit the experimental data.

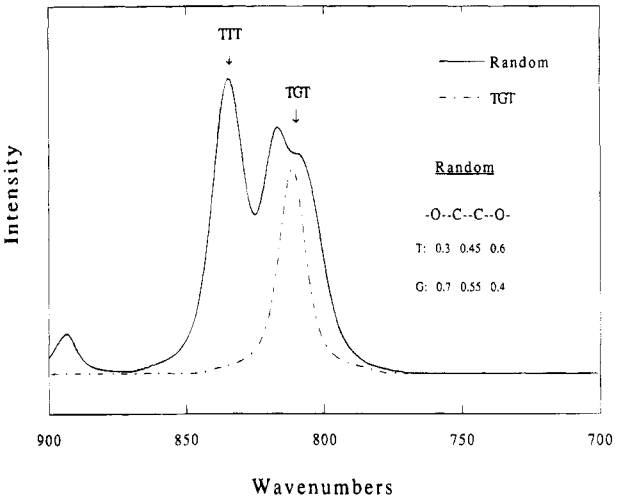

Figure 7. Calculated spectra of (*S*)-DMP obtained for a random conformational distribution and for the TG$_\alpha$T conformation in the 700−900 cm^{-1} range.

Table 4. Energy of the Bands in the 800−900 cm^{-1} Region for Various Conformations Calculated by Normal Coordinate Analysis for $CH_3O-(CH(CH_3)CH_2O-)_n-CH_3$

n	sequence[a]	conformation	wavenumbers
1		TTT	835
		TG$_\alpha$T	812
		TG$_\beta$T	799
		G$_\alpha$G$_\alpha$T	818
		G$_\beta$G$_\alpha$T	815
3	H−T−H−T	(TTT)$_3$	861, 847, 825
		(TG$_\alpha$T)$_3$	870, 839, 806
	H−T−H−H	TG$_\alpha$TTG$_\beta$TTG$_\alpha$T	842, 810
		TG$_\alpha$TTG$_\alpha$TTG$_\beta$T	857, 814, 800
4	(H−T)$_3$	(TTT)$_4$	862, 856, 841, 823
		(TG$_\alpha$T)$_4$	875, 856, 830, 806
7	(H−T)$_6$	(TTT)$_7$	863, 862, 858, 852, 842, 831, 822
		(TG$_\alpha$T)$_7$	880, 873, 862, 848, 833, 820, 806

[a] H: head. T: tail.

The normal mode calculation was extended to MPPO having chemical repeat units of (*S*)-configuration. The fundamental frequencies obtained by calculation in the 800−900 cm^{-1} region are given in Table 4. The characteristic band of the TG$_\alpha$T conformation at 806 cm^{-1} (811 cm^{-1} for 1,2-dimethoxypropane) is clearly separated from bands associated with other conformations, particularly the TTT conformation. The calculated band position of the TG$_\alpha$T conformation obtained for MPPO having more than two units of propylene oxide was found to change slightly (a few wavenumbers) depending on the conformation of the neighbor bonds or structural defects such as head-to-head sequences in our calculation. The band in the 805−810 cm^{-1} range can only be associated with a TG$_\alpha$T conformation of the −O−C−C−O− bond, regardless of chain length.

As can be seen from Figures 3 and 7, the experimental data for both frequency and intensity can be simulated

extremely well by chains having a conformational distribution such as in Figure 7. On the basis of the simulated spectra, observed bands of 1,2-dimethoxypropane centered at 836 and 807 cm^{-1} are assigned to TTT and $TG_\alpha T$ conformations, respectively. As mentioned above, the strong band at 811 cm^{-1} in the DMP–$LiClO_4$ complex can definitely be assigned to the $TG_\alpha T$ conformation since the experimental and calculated spectra superimpose nearly exactly. Therefore we conclude that the intensity increase of this band when salt is added is attributed to the increase in the $TG_\alpha T$ conformation population induced by interaction between the lithium cation and ether oxygens. This result indicates that the lithium cation prefers to interact with the gauche α conformation of the –C–C– bond. In the absence of salt, the conformational distribution of either PPO or 1,2-dimethoxypropane is broad and therefore the corresponding Raman spectra also exhibit broad overlapping bands. When salt is added, the interaction between the lithium cation and ether oxygen narrows the conformational distribution and thus the $TG_\alpha T$ conformation is dominant. As expected, the band associated with this conformation then emerges as the principal band in the 800 cm^{-1} region. This assignment can be extended to both HPPO and MPPO systems. As mentioned above, the band frequency assignable to the $TG_\alpha T$ conformation of the –O–C–C–O– bond can be changed by a few wavenumbers depending on the conformation of neighboring –O–C–C–O– units.

The small energy (frequency) difference in the bands observed in 1,2-dimethoxypropane or PPO versus their corresponding salt complexes can be explained in two ways. First, the frequency shift can be attributed to the change in the valence force field by salt addition. Or, as already experienced by calculation, it can simply be caused by overlapping of broad bands because the exact band position for a certain conformation can be perturbed by the contribution from others when molecules have a broad chain conformational distribution. Our case is close to the latter. In our calculation, we did not take into account the possibility of changes in force constants induced by salt interactions. Since the experimental data can be explained by our calculated results, even with small changes in the force field, the effects do not appear significant, at least for vibrational modes in the 800 cm^{-1} region.

Conclusions

We in this study applied normal coordinate analysis to 1,2-dimethoxypropane and methoxy-terminated PPO in order to investigate the chain conformational dependence of Raman bands in the disordered state. We then characterized changes in the conformational distribution of PPO in the presence of $LiClO_4$. An isotropic Raman spectrum for 1,2-dimethoxypropane can be generated by calculation in the 700–900 cm^{-1} region. By comparison of calculated isotropic Raman spectra with experimental results, the characteristic band at 810 cm^{-1} increasing in intensity with salt concentration has been assigned to the $TG_\alpha T$ conformation. Studies were extended to MPPO up to 7-mer and consistent results obtained. It was found that the interaction between the lithium cation and ether oxygen predominantly contributes to formation of the gauche α conformation of –C–C– bonds along the backbone. The chain conformational distribution of PPO has been changed to the distribution having increased gauche α conformations of C–C bonds by interaction of Li^+ and ether oxygen. As confirmed in Fourier transform Raman spectra obtained for an extensive PPO molecular weight range along with calculated results, the characteristic band around 810 cm^{-1} represents a common conformation ($TG_\alpha T$) in local bonds of –O–C–C–O– regardless of chain length. Therefore this assignment can be used for information concerning the relative content of the $TG_\alpha T$ conformation of propylene oxide units in any PPO system.

Acknowledgment. This project has been supported by a grant from Army Research Office, Grant No. DAAH04-95-1-0126, and the STTR program.

References and Notes

(1) *Polymer Electrolyte Reviews*; MacCallum, J. R., Vincent, C. A., Eds.; Elsevier Applied Science: London, 1987; Vol. 1.
(2) *Polymer Electrolyte Reviews*; MacCallum, J. R., Vincent, C. A., Eds; Elsevier Applied Science: London, 1989; Vol. 2.
(3) Lee, C. C.; Wright, P. V. *Polymer* **1982**, *23*, 681.
(4) Payne, D. R. *Polymer* **1982**, *23*, 690.
(5) McLin, M. G.; Angell, C. A. *J. Phys. Chem.* **1991**, *95*, 9464.
(6) Torell, L. M.; Schantz, S. *J. Non-Cryst. Solids* **1991**, *131–133*, 981.
(7) Watanabe, M.; Ikeda, J.; Shinohara, I. *Polym. J.* **1983**, *15*, 175.
(8) Watanabe, M.; Ikeda, J.; Shinohara, I. *Polym. J.* **1983**, *15*, 65.
(9) Watanabe, M.; Ogata, N. *Br. Polym. J.* **1988**, *20*, 181.
(10) Vachon, C.; Vasco, M.; Perrier, M.; Prud'homme, J. *Macromolecules* **1993**, *26*, 4023.
(11) Takahashi, H.; Kyu, T.; Tran-Cong, Q.; Yano, O.; Soen, T. *J. Polym. Sci., Part B* **1991**, *29*, 1419.
(12) Papke, B. L.; Ratner, M. A.; Shriver, D. F. *J. Phys. Chem. Solids* **1981**, *42*, 493.
(13) Maxfield, J.; Shepherd, I. W. *Polymer* **1975**, *16*, 505.
(14) Matsuura, H.; Fukuhara, K. *J. Mol. Struct.* **1985**, *126*, 251.
(15) Koenig, J. L.; Angood, A. C. *J. Polym. Sci., Polym. Phys. Ed.* **1970**, *8*, 1787.
(16) Frech, R.; Manning, J.; Teeters, D.; Black, B. E. *Solid State Ionics* **1988**, *28–30*, 954.
(17) Frech, R.; Manning, J.; Black, B. *Polymer* **1989**, *60*, 1785.
(18) Manning, J.; Frech, R.; Hwang, E. *Polymer* **1990**, *31*, 2245.
(19) Manning, J.; Frech, R. *Polymer* **1992**, *33*, 3487.
(20) Schantz, S.; Torell, L. M.; Stevens, J. R. *J. Appl. Phys.* **1988**, *64*, 2038.
(21) Snyder, R. G. *J. Chem. Soc., Faraday Trans.* **1992**, *88*, 1823.
(22) Painter, P. C.; Coleman, M. M.; Koenig, J. L. *The theory of vibrational spectroscopy and its application to polymeric materials*; John Wiley & Sons: New York, 1982.
(23) Wilson, E. B.; Decius, J. C.; Cross, P. C. *Molecular Vibrations*; Dover Publications, Inc.: New York, 1955.
(24) Snyder, R. G.; Kim, Y. *J. Phys. Chem.* **1991**, *95*, 602.
(25) Hallmark, V. M.; Bohan, S. P.; Strauss, H. L.; Snyder, R. G. *Macromolecules* **1991**, *24*, 4025.
(26) Abe, A.; Hirano, T.; Tsuruta, T. *Macromolecules* **1979**, *12*, 1092.
(27) Schachtschneider, J. H.; Snyder, R. G. *Spectrochim. Acta* **1963**, *19*, 117.
(28) Schachtschneider, J. H.; Snyder, R. G. *J. Polym. Sci., Part C* **1964**, 99.
(29) Snyder, R. G. *J. Mol. Spectrosc.* **1960**, *4*, 411.
(30) Snyder, R. G. *J. Mol. Spectrosc.* **1961**, *7*, 116.
(31) Snyder, R. G.; Schachtschneider, J. H. *Spectrochim. Acta* **1963**, *19*, 85.
(32) Hirano, T.; Miyajima, T. *J. Mol. Struct.* **1985**, *126*, 141.
(33) Abe, A.; Tasaki, K. *J. Mol. Struct.* **1986**, *145*, 309.
(34) Miyajima, T.; Hirano, T.; Sato, H. *J. Mol. Struct.* **1984**, *125*, 97.
(35) Snyder, R. G.; Zerbi, G. *Spectrochim. Acta* **1967**, *23A*, 391.
(36) Scherer, J. R.; Snyder, R. G. *J. Chem. Phys.* **1980**, *72*, 5798.
(37) Snyder, R. G.; Schachtschneider, J. H. *Spectrochim. Acta* **1965**, *21*, 169.
(38) Snyder, R. G. *J. Chem. Phys.* **1982**, *76*, 3921.
(39) Snyder, R. G. *Macromolecules* **1990**, *23*, 2081.
(40) Snyder, R. G.; Strauss, H. L. *J. Chem. Phys.* **1987**, *87*, 3779.
(41) Aroney, M. J.; Le Fevre, R. J. W.; Ritchie, G. L. D.; Saxby, J. D. *Aust. J. Chem.* **1967**, *20*, 375.
(42) Denbigh, K. G. *Faraday Soc. Trans.* **1940**, *36*, 936.
(43) Grough, K. M. *J. Chem. Phys.* **1989**, *91*, 2424.
(44) Kawasaki, A.; Furukawa, J.; Tsuruta, T.; Saegusa, T.; Kakogawa, G.; Sakata, R. *Polymer* **1960**, *1*, 315.

MA946225+